Journal of
Materials Chemistry A

Accepted Manuscript

This is an *Accepted Manuscript*, which has been through the RSC Publishing peer review process and has been accepted for publication.

Accepted Manuscripts are published online shortly after acceptance, which is prior to technical editing, formatting and proof reading. This free service from RSC Publishing allows authors to make their results available to the community, in citable form, before publication of the edited article. This *Accepted Manuscript* will be replaced by the edited and formatted *Advance Article* as soon as this is available.

To cite this manuscript please use its permanent Digital Object Identifier (DOI®), which is identical for all formats of publication.

More information about *Accepted Manuscripts* can be found in the **Information for Authors**.

Please note that technical editing may introduce minor changes to the text and/or graphics contained in the manuscript submitted by the author(s) which may alter content, and that the standard **Terms & Conditions** and the **ethical guidelines** that apply to the journal are still applicable. In no event shall the RSC be held responsible for any errors or omissions in these *Accepted Manuscript* manuscripts or any consequences arising from the use of any information contained in them.

Functionalized Meso/Macro-Porous Single Ion Polymeric Electrolyte for Applications in Lithium Ion Batteries

Rupesh Rohan[1], Yubao Sun[2]*, Weiwei Cai[1], Kapil Pareek[1], Yunfeng Zhang[1], Guodong Xu[1], Hansong Cheng[1,2]*

[1]Department of Chemistry, National University of Singapore, 3 Science Drive3, Singapore - 117543

[2]Sustainable Energy Laboratory, China University of Geosciences Wuhan, 388 Lumo RD, Wuhan 430074, China

ABSTRACT: We report a method to significantly enhance conductivity of lithium ions in a polymeric lithium salt membrane by introducing functionalized meso/macro-pores to accommodate a mixture of organic solvents in the polymer matrix. The meso/macro-porous membrane is formed by a lithium poly[4-styrenesulfonyl(phenylsulfonyl)imide] polymer and serves as an electrolyte in lithium ion batteries. The substantially enhanced ionic conductivity of the membrane arises from the facile release of the lithium ions to the solvent and the extensive interconnectivity of the meso/macro-pores that provides a smooth passage for the solvated lithium ions to transport. The fabricated meso/macro-porous polymer membrane displays excellent high-temperature sustainability and wide electrochemical stability, important for battery safety and enhancement of device performance and longevity. The performance of the membrane is demonstrated in an assembled Li-ion battery cell.

Keywords: Electrolyte, separator, meso /macro-porous, single ion, lithium ion battery.

1. Introduction

The abundant clean energies, such as wind, hydro and solar energies, are the ultimate sources to cope with the present energy crisis and environmental challenge worldwide. These sources, however, are unable to provide an on-call service and intermittents, such as capacitors and batteries, are needed to store and supply energies on demand. [1-4] For portable and daily

Journal of Materials Chemistry A Accepted Manuscript

usage of electronic devices, lithium ion [5-7] and lithium polymer [8-10] batteries are among the most commonly used energy storage systems.[11] For development of lithium ion batteries, one of the critical technical challenges is to improve the key performance regulatory parameters, including ionic conductivity and transference number of cations, which has been a subject of intense research efforts.[4, 12, 13] Ionic conductivity can be improved by increasing the degree of dissociation between lithium ions and electrolytes as well as by providing resistance free passage for ion transport, whereas transference number of cations can be potentially enhanced to unity by introducing rigid anionic species in solid framework.[14]

Solid polymer electrolyte (SPE) based lithium ion batteries are known to be safer and more durable than the liquid lithium salt based batteries.[15-17] These electrolytes are composed of lithium ion salts blended with various polymer networks to form membranes, which serve both as an electrolyte and as a separator in a battery device.[18, 19] A conventional SPE works in a solvent-free environment and largely depends on an ion-coupled mechanism (hopping of Li ions through segmental movements of polymers) for Li ions to shuttle between electrodes.[20-22] Unfortunately, to date, most SPEs are unable to provide sufficiently high ionic conductivity on the order of 10^{-3} Scm^{-1} at a near ambient temperature.[23] To overcome the difficulty of the inherently low ionic conductivity of conventional SPEs, the concept of single ion conducting gel polymer electrolyte (SIPE) was recently proposed.[24, 25] These SIPEs provide several advantages over the liquid lithium salt electrolytes and the conventional SPEs, both of which behave as dual-ion conductors upon charging and discharging. [26] The SIPEs not only provide high ionic conductivity but also eliminate the problem of concentration polarization.[18, 26] The membranes of the electrolytes normally consist of a polymer electrolyte salt as well as low temperature flexible polymers serving as a binder.[24, 27, 28] With a proper porosity in the membranes, organic solvents can be accommodated to form a gel-electrolyte to enhance the ionic conductivity. The commonly used organic solvents include ethyl carbonate (EC), propyl carbonates (PC), etc.[12, 29] In contrast to the conventional SPEs, in which ion conduction is realized via a hoping mechanism, [24, 30, 31] high ionic conductivity in SIPEs can be achieved both through charge separation arising from the electron delocalization of the anionic species and through the liquid media. For example, Kerr et al. synthesized a single ion conductor based on lithium bis(allylmalonato)borate (LiBAMB) and comb-branched polyepoxide ether to

Journal of Materials Chemistry A Accepted Manuscript

serve as an electrolyte and demonstrated significant battery performance at room temperature[32, 33] Remarkably, they found that the ionic conductivity was increased by 2 orders of magnitude in the SIPE membrane with an organic solvent over in a dry polyelectrolyte. Recently, we reported successful synthesis and fabrication of a class of boron based SIPE membranes with substantially higher ionic conductivity than what was observed in conventional SPEs.[34] These compounds exhibit good thermal stability, with ionic conductivity comparable to that of liquid electrolytes. Unfortunately, the porosity of the membranes is relatively small so that the amount of organic solvent accommodated in the membranes may not be sufficient to induce even higher ionic conductivity.[35-37]

To explore the utility of the single ion polymer electrolyte concept and to take advantages of the porosity of the material synchronously in a single system for Li-ion battery applications, we present in this paper a novel procedure of synthesizing a polystyrene-based single ion porous polymeric electrolyte and demonstrate its cyclic battery performance. This material exhibits high polarization provided by anionic functional groups with delocalized charges exposed on surfaces of the inter-connected meso/macro-pores of the polymeric framework and Li^+ ions weakly associated with the polymer via an ionic bond. Organic solvents conventionally used in Li-ion batteries, such as PC and EC, are then accommodated in the meso/macro-pores to facilitate transport of the Li^+ ions. As an expected outcome, this electrolyte shows high room temperature conductivity on the order of 10^{-3} Scm^{-1}, approximately one order of magnitude higher than that of the non-porous electrolyte made of the same material. The high ionic conductivity of the SIPE membranes offers a potential opportunity to develop less expensive, safer and more flexible Li-ion batteries.

2. Experimental

2.1. Materials

Styrene (Alfa-Aesar), divinylbenzene (Alfa-Aesar), tetraethoxysilane (Alfa-Aesar 99%), polyvinylidene fluoride (PVDF) (Solef 6020), Mw 680,000 g mol^{-1} (Solvay), benzoyl peroxide (BPO) (MerckSchuchardt*),* dimethylaminopyridine (DMAP) (Sigma-Aldrich), triethylamine (Fisher), sodium hydroxide (Chemcon 40%), chlorosulfonic acid (Fluka), thionyl chloride (Tee Hai), hydrofluoric acid (Fisher 60%), benzenesulfonamide (Sigma-Aldrich), lithium hydroxide monohydrate (Sigma-Aldrich), dichloroethane (DCE) (Alfa-Aesar 99%), dichloromethane (DCM) (Fisher), ethanol (Fisher), acetonitrile (Tedia), lithium

Journal of Materials Chemistry A Accepted Manuscript

iron phosphate (Sigma-Aldrich), N-methyl-2-pyrrolidone (NMP) (VWR), di-ionized water (molar resistivity 18 MΩ cm^{-1}). All reagents were of analytical grade. Styrene and divinylbenzene were washed with sodium hydroxide aqueous solution (5 wt %) to remove the inhibitor, and then distilled under a reduced pressure prior to polymerization.

2.2. Methods

All infrared spectra were taken with a Bio-Rad Excalibur FT-IR Spectrometer in the 400-4000 cm^{-1} frequency range. The microstructures of the polymer electrolyte were probed using the field emission scanning electron microscopy (FESEM) with JEOL JSM-6701F. Samples were prepared by platinum sputtering under 9 Pa at room temperature (20s, 30mA) with JEOL JFC-1600 Fine Coater. Thermal degradation study was performed under inert atmosphere of N_2 (flow rate 60 cm^3min^{-1}) at 10 ^oC min^{-1} heating rate in Thermo Gravimetric Analyzer (TGA Q 50) of TA, Inst., USA. The experiment was conducted from room temperature to 1000 ^oC. The differential scanning calorimetry (DSC) study was carried out on Differential Scanning Calorimeter (DSC-1 Star System) of Mettler Toledo, USA, under an inert atmosphere of N_2 (flow rate 60 cm^3min^{-1}) from 30 ^oC to 250 ^oC for 3 cycles at the heating/cooling rate of 10 ^oC min^{-1}. The cross-polarized magic-angle-spinning (CP-MAS) solid state ^{13}C NMR was performed on Bruker DRX 400 instrument. Pore size distribution (PSD) and N_2 adsorption-desorption isotherms at 77K were measured by Micromeritics ASAP 2020.

The ionic conductivity of the polymer electrolytes was measured by electrochemical impedance spectroscopy (EIS) using a Electrochemical Workstation (ZHENNIUM) of Zahner-Elektrik GmbH & Co., Germany, with the EIS module over the frequency range of 4×10^6 to 1 Hz with the oscillating voltage of 5 mV. The electrolyte membrane was placed inside a cylindrical stainless steel device with a cavity of 1.5 cm diameter. The measurement device was sealed in a glove box under argon and heated at 80 ^oC in an oven to obtain a maximum contact between the membrane and the surface of the device prior to analysis. The temperature vs conductivity graph was obtained by heating followed by cooling the device in the testing temperature range from 90 ^oC to room temperature downwards. The Nyquist curves of the real (Z') vs imaginary (Z'') parts of the impedance were fitted with the 'SIM' software.

Journal of Materials Chemistry A Accepted Manuscript

To analyse the battery performance, a multichannel battery testing instrument Arbin BT-2000 was used for the discharge capacity measurement of the coin cells assembled with the synthesized polymeric electrolyte membrane. The composite cathode was prepared by casting a well stirred solution of $LiFePO_4$ (75%), PVDF (10%), acetylene black (10%) and a small amount of lithium bis(4-carboxy phenyl sulfonyl)imide (5%) as a supporting electrolyte in a NMP solvent on to an aluminum foil.The resulting electrode was dried in a vacuum oven at 80 ^oC for 12 hours. The dried cathode was then cut into a circular shape used in coin cells. The assembling of the standard coin cells (CR2025) was done inside a glove box.

2.3 Synthesis

2.3.1. Synthesis of silica nano-particles

Mono-dispersed SiO_2 nanoparticles with the mean diameter of 260 nm were prepared by hydrolysis of TEOS in an alcoholic medium in the presence of water and ammonia similar to the reported procedure by Stober et al.[38, 39] In the synthesis, a solution with a given amount of water, ethanol and ammonia was introduced into a three-neck round flask of 250 ml at room temperature, stirring at a mild rate. Then, tetraethoxysilane (TEOS) was introduced continuously in the medium at a precise rate. The reaction took place at room temperature under continuous stirring for over 12 hours. After the hydrolysis reaction was completed, the mixture contained about 2 wt% SiO_2 particles and these particles were collected by centrifugation from the white suspension. The primary sample of silica spheres was obtained. In order to obtain good quality mono-dispersed spheres, the primary silica sphere sample was re-dispersed in ethanol using an ultrasonicator, and was recollected by centrifugation. The above washing process was repeated three times. The final product was dispersed in ethanol to obtain a 4 wt% SiO_2 disperson. A thin layer of SiO_2 particles, packed in hexagonal cubic packing (hcp), was made between two glass plates by capillary action followed by evaporation of ethanol. Drying was done at room temperature, which took 2-3 days.

2.3.2. In-situ polymerization and etching

The synthetic process is shown schematically in Scheme 1. After drying, the SiO_2 pattern was transferred into a tube containing 1.70 ml of styrene, 0.30 ml of divinylbenzene (DVB) and 0.02 g of benzoyl peroxide (BPO) for one hour to facilitate the filling of the gap between the glass slides. Subsequently, the tube was transferred to an oven for 24 hours at 90 ^oC to ensure complete polymerization. The post-polymerized template, which contains a poly-

Journal of Materials Chemistry A Accepted Manuscript

styrene/DVB membrane, was immersed in a HF solution for seven days to ensure clean etching of the SiO_2 particles and glass plates.[40-42] The HF treated cross-linked porous membrane was washed by distilled water thoroughly and dried.

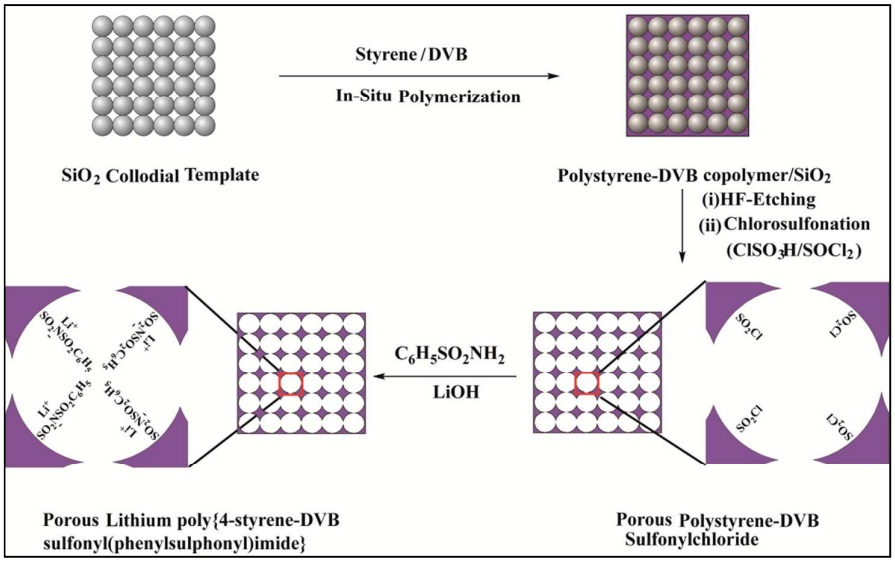

Scheme1. Schematic representation of the synthetic protocol of the functionalized meso/macro-porous polystyrene/DVB membrane.

2.3.3. Synthesis of lithium poly[4-styrenesulfonyl(phenylsulfonyl)imide] (PSSPSI) porous membrane

The grafting of sulfonyl(phenylsulfonyl)imide group on the porous membrane was done in two steps. In the first step, chlorosulfonation of polystyrene/DVB membrane took place in the presence of chlorosulfonic acid and thionyl chloride (both in excess), in DCE medium at 40 ^oC for 2 hours. Washing was done by DCE followed by acetonitrile until the pH increased to 7. The membrane was dried for 6 hours at 80 ^oC. FTIR (ATR cm^{-1}): υ = 1656(ν_{CC}), 1383 (νas_{SO2}), 1128 (νs_{SO2}).[43-45]{*ν:* stretching, *α* and *β:* in plane deformation *s:*symmetrical, *as:* asymmetrical }. Elemental analysis: calculated: C, 49.86; H, 3.66; S, 14.97; Cl, 16.56 %, found: C, 47.88; H, 4.11; S, 14.76; Cl, 9.96 %. Degree of sulfonation: ca. 90%. Degree of chlorosulfonation: ca. 67%. In the second step, imidification was done according to the procedure described in references 16 and 23. 6 ml of triethylamine, 3 g of benzenesulfonamide and 2.12 g of DMAP were added into a flask containing 30 ml of acetonitrile solvent, and the solution was stirred for an hour under argon atmosphere to

Journal of Materials Chemistry A Accepted Manuscript

solubilize all ingredients. Then, the chlorosulfonated polystyrene/DVB membrane (0.5 g) was immersed in the solution for 16 hours at 60 ^{o}C. Subsequently, the membrane was washed with an excess of acetonitrile solvent till the pH increased to 7. This membrane was kept in a saturated aqueous solution of lithium hydroxide at 70 ^{o}C for 4 hours for lithiation. Washing was completed with distilled water until the pH was reduced to 7. The membrane was dried under vacuum at 80 ^{o}C for 24 hours prior to transferring to a glove box. FTIR (ATRcm^{-1}): υ =1641(ν_{CC}), 1413(β_{CH}+ν_{CC}), 1384 (νas_{SO2}), 1128 (νs_{SO2}), 1027(ν_{CS}), [23, 46, 47].CP-MAS ^{13}C NMR δ ppm 148.82, 145.32, 141, 127.07, 41.24. Elemental analysis: calculated: Elemental Analysis: Calculated: C, 51.06; H, 3.67; N, 4.25; S, 19.47; Li, 2.11 %. Found: C, 39.77; H, 5.76; N, 1.09; S, 12.03; Li, 1.92 %. Degree of imidification: ca. 38%.

2.3.4. Formation of the electrolyte membrane

0.039 g PVDF (vacuum dried at 40 ^{o}C for 24 hours) was transferred to a 5 ml glass beaker followed by addition of 0.15 ml EC/PC (volume ratio is 1:1). A magnetic stirrer was also placed in the beaker and the mixture was stirred at 60 ^{o}C for several minutes. The resulting viscous solution was poured into another beaker where 0.040 g of the broken porous lithium poly[4-styrenesulfonyl(phenylsulfonyl)imide] (P-PSSPSI) membrane pieces was placed. The resulting mixture was heated on a hot plate at 100 ^{o}C for a few minutes and then cooled down. Upon cooling, the formed membrane could be readily peeled off from the beaker. The entire experiment was performed inside a glove box under argon gas atmosphere. This PVDF binded P-PSSPSI (BP-PSSPSI) membrane was further used for conductivity measurement and battery fabrication.

3. Result and Discussion

3.1 Synthesis and characterization of the P-PSSPSI membrane

As shown schematically in Scheme 1, styrene with divinylbenzene (DVB), which serves as a cross-linking agent, on a silica particle template were used as the precursors. Upon polymerization followed by etching of hexagonally packed (hcp) silica particles with a size ranging from 260 to 300 nm, a porous 30 μm thick membrane with open and interconnected meso and macro pores was formed (Figs. 1a and 1b). The size of the macro pores is dictated by the diameter of silica particles, while the meso pores are formed due to the etching of the contact surfaces of the silica particles in the hcp packing. Upon chlorosulfonation followed by imidfication of polystyrene/DVB membrane, the resultant P-PSSPSI membrane retains its macro pores as confirmed by the SEM image shown in Fig.1c. Unfortunately, the inherent

Journal of Materials Chemistry A Accepted Manuscript

brittleness of the polystyrene-DVB copolymer and high porosity make this membrane prone to cracks and mechanically less robust. To overcome this difficulty, small pieces of the membrane were cemented with a solution of PVDF in EC/PC 1:1 (v/v). A crack-free, flexible membrane was obtained. The membrane also retains the feature of open and interconnected macro pores as shown in Fig. 1d.

The DFT pore size distribution curves calculated from N_2 adsorption-desorption isotherms at 77 K for both the P-PSSPSI membrane and the BP-PSSPSI membrane are shown in Fig. 2a and 2b, respectively. The distribution curves show that both the P-PSSPSI and the BP-PSSPSI membranes possess a range of meso pores, in addition to macro pores. Figure 2 indicates that no significant change occurs in the porosity upon cementing the segments of the P-PSSPSI membrane.

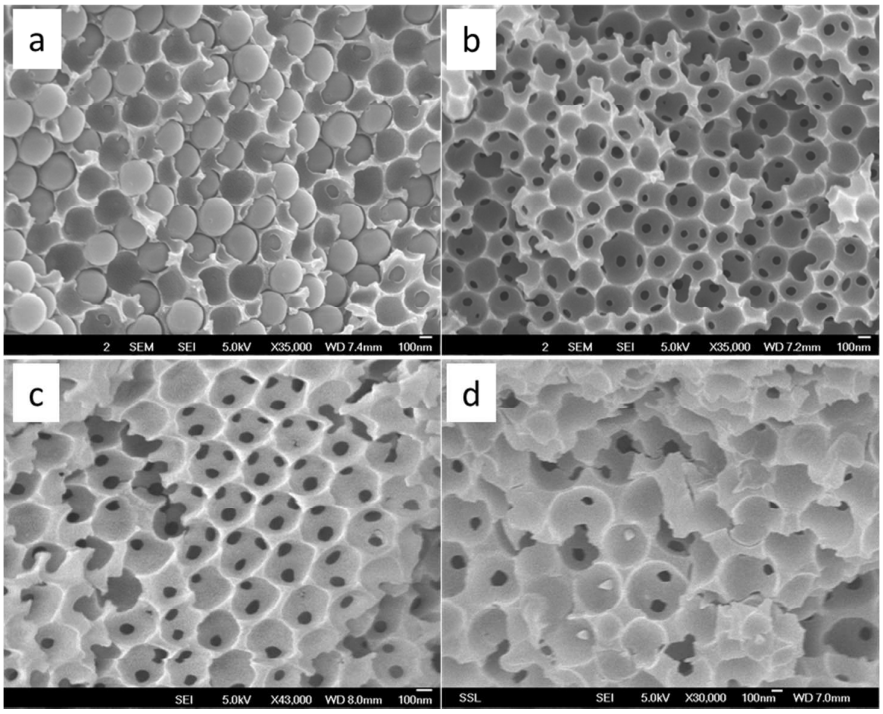

Figure 1. The SEM images of the polystyrene-DVB membrane: (a) before etching, (b) after etching, (c) after functionalization and (d) after functionalization and binding with PVDF.

Journal of Materials Chemistry A Accepted Manuscript

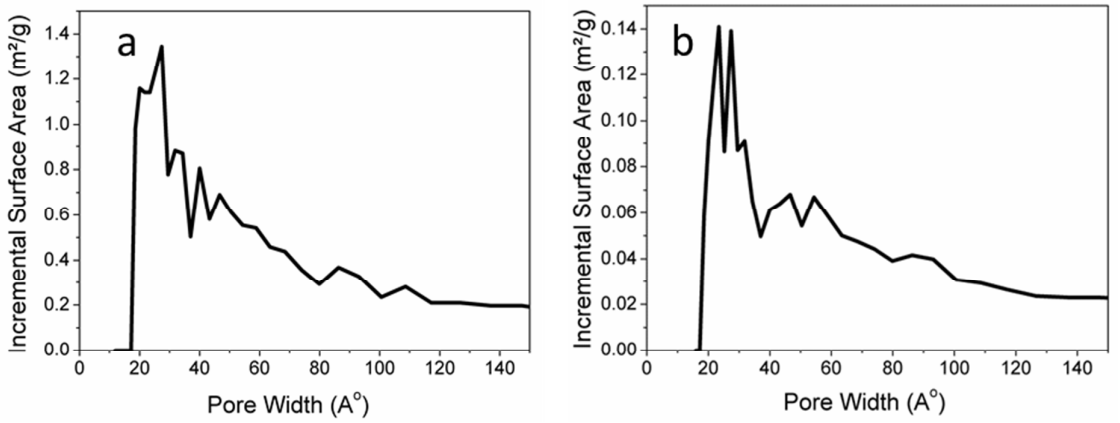

Figure 2. DFT pore size distribution calculated from N_2 adsorption-desorption isotherms at 77K for (a) the P-PSSPSI membrane, (b) the BP-PSSPSI membrane.

The two-step chemical synthesis of the PSSPSI membrane was confirmed by FTIR, CP-MAS solid state ^{13}C NMR and elemental analysis (EA) techniques. The sulfur and chlorine contents found by EA testing after the first step correspond to 90% sulfonation followed by 67 % chlorosulfonation of the polystyrene-DVB membrane. The nitrogen content detected after the second step confirms 38% imidification of the chlorosulfonated membrane. The relatively small degree of imidification indicates that the imidification was achieved only on the walls of the pores as expected.

The TGA thermograms of the P-PSSPSI membrane and the BP-PSSPSI membrane are shown in Fig.3. For the P-PSSPSI membrane, a small reduction of 6% of the initial mass is observed due to the loss of solvent and moisture. The first stage thermal degradation begins at 420 ^{o}C and extends up to 480 ^{o}C (ca. 8% of weight loss), corresponding to the degradation of non-functionalized polystyrene.[48] The second stage occurring in 500 -600 ^{o}C (ca 55% of weight loss) correlates with the degradation of the functionalized polystyrene (cleavage of the C-S bonds).[23] The BP-PSSPSI membrane also shows the similar trend of degradation. However, the second stage degradation occurs in a relatively lower temperature range (430-530 ^{o}C) than the former, predominantly due to the loss of PVDF component of the membrane, which thermally degrades just above 400 ^{o}C.[49, 50] The result confirms the high thermal stability of both the P-PSSPSI and the BP-PSSPSI membranes at elevated temperatures and suggests that the material could also be potentially useful for high temperature applications of batteries.

Journal of Materials Chemistry A Accepted Manuscript

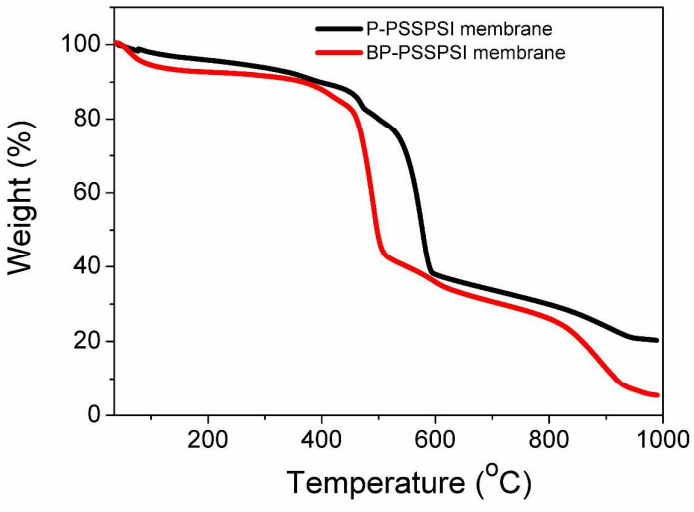

Figure 3. The TGA thermograms of the P-PSSPSI membrane and the BP-PSSPSI membrane (N_2, 10 °C /min, RT to 1000 °C).

The DSC thermograms of the P-PSSPSI membrane, the neat PVDF and the BP-PSSPSI membrane are shown in Fig. 4. The glass transition temperature (T_g) of the P-PSSPSI was found to be 160 °C. The high T_g arises mainly from the bulky rigid benzene rings in the main chains. The DSC thermogram of the neat PVDF shows an endothermic peak at 171 °C, corresponding to its melting point. As depicted in the DSC thermogram of the BP-PSSPSI membrane, no T_g was found, which may be attributed to the overlapping of the expected temperature range of T_g with the melting point temperature range of PVDF. In addition, the peak corresponding to the melting point of PVDF does not shift appreciably in the BP-PSSPSI, which indicates that except a small physical interaction, no strong adhesive force works between PVDF and P-PSSPSI, and PVDF serves only as a binder.

Journal of Materials Chemistry A Accepted Manuscript

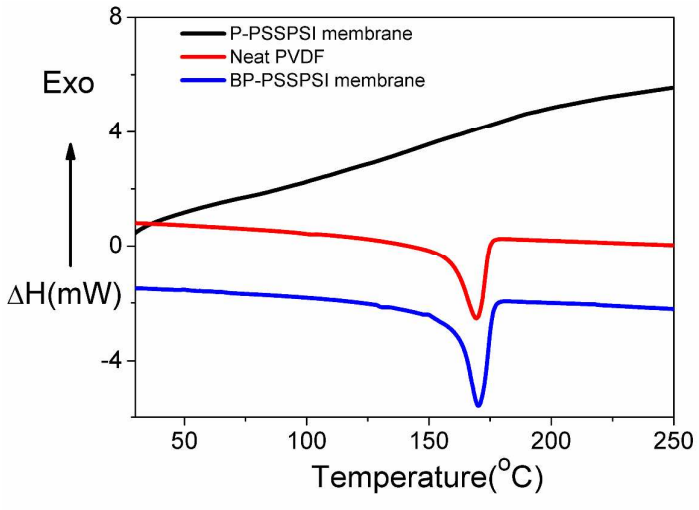

Figure 4. The DSC thermograms of the P-PSSPSI membrane, the neat PVDF and the BP-PSSPSI membrane (N_2, 10 °C /min, RT to 250 °C).

3.2. Electrochemical Properties

The polymer electrolyte membrane cemented with PVDF was cut into a circular shape for EIS testing. The ionic conductivity was calculated using the equation

$$\sigma = \frac{l}{Ra}$$

where σ is the conductivity of the membrane, and l, R and a represent the thickness of the membrane, the bulk resistance and the area of the membrane, respectively. To understand the influence of the porosity of the electrolyte membrane, another electrolyte membrane was prepared using the same precursors but without use of the silica template. The resultant product was a brittle dense membrane (D-PSSPSI) and thus had to be cemented by the same method using the PVDF solution in EC/PC. The EIS responses of the cemented electrolyte membranes at room temperature with and without porosity in the Nyquist coordinates are shown in Fig. 5, where the equivalent circuit used for the fitting is also depicted. Here, R1, R2, CPE and W stand for the bulk resistance, the interfacial resistance, the constant phase element and the Warburg resistance, respectively. The PVDF binded D-PSSPSI (BD-PSSPSI) membrane shows a much higher impedance value (Z') than the BP-PSSPSI membrane in the mid frequency range. The Z' value in this frequency range predominantly

Journal of Materials Chemistry A Accepted Manuscript

corresponds to the interfacial resistance R2 and thus significantly affects battery performance.[51]

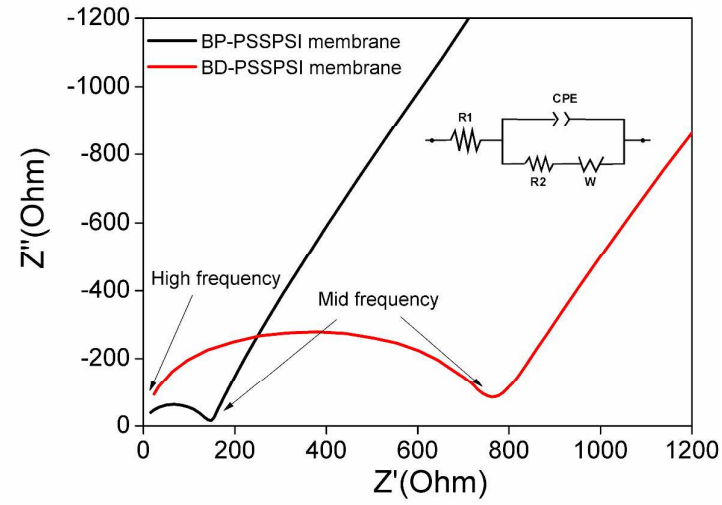

Figure 5. The EIS plots of the BP-PSSPSI and the BD-PSSPSI membranes at room temperature. The inset is the corresponding equivalent circuit.

The ionic conductivity of the P-PSSPSI membrane was found to be 6.3×10^{-3} S cm^{-1} in an organic solvent using EC/PC of 1:1 v/v at room temperature. The temperature-dependency of the ionic conductivity for the BP-PSSPSI and the BD-PSSPSI membranes is shown in Fig. 6. The plot of log value of the ionic conductivity of the BP-PSSPSI and the BD-PSSPSI membranes vs. the inverse of absolute temperature displays consistency with a typical Arrhenius curve within the test temperature range from room temperature to 90 ^{o}C. The room temperature conductivity of the BP-PSSPSI membrane was found to be 4.0×10^{-3} S cm^{-1}, only modestly smaller than the value of the P-PSSPSI. The ionic conductivity of the membrane is among the highest values of the single ion polymer electrolytes reported to date and close to the conductivity of liquid electrolytes.[52] The highest measured conductivity at 90 ^{o}C is 1.0×10^{-2} S cm^{-1}. As expected, the measured conductivity shows a monotonic increase with temperature; the conductivity increment is essentially linear but not as steep as in small molecular electrolyte or ionic based gel polymer electrolytes.[30, 53] The modest increment may be attributed to the mechanical coupling between ion transport and polymer host mobility at a given temperature according to the free volume theory of polymers.[23, 54] The remarkably high ionic conductivity is attributed to the high porosity of the membrane as well as to the high acidity of sulfonyl(phenylsulfonyl)imide group, which facilitates transport

Journal of Materials Chemistry A Accepted Manuscript

of Li ions in the solvent readily. For the BD-PSSPSI membrane, the room temperature conductivity was found to be 5.7×10^{-4} S cm^{-1}, substantially smaller than the conductivity of the BP-PSSPSI membrane, which underscores the importance of porosity of battery electrolyte membranes for enhancement of ionic conductivity.

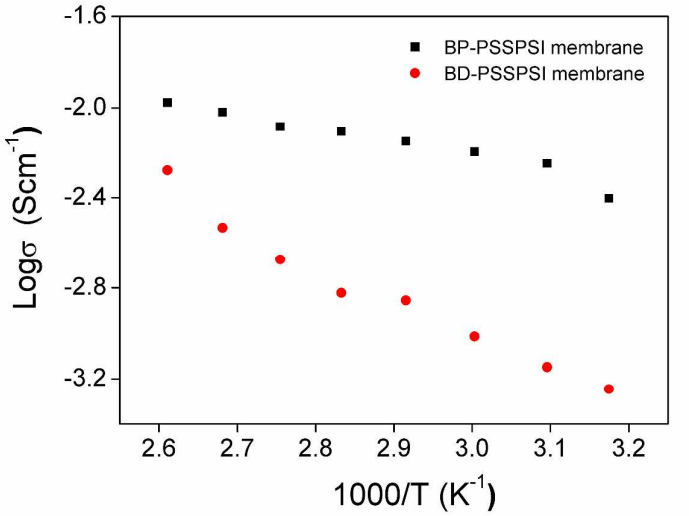

Figure 6. The Arrhenius plot of log ionic conductivity vs. inverse of absolute temperature for the BP-PSSPSI and the BD-PSSPSI membranes.

3.3 Battery performance

To demonstrate the battery performance of the BP-PSSPSI membrane, we assembled several coin cells using $LiFePO_4$ as the cathode and a lithium foil as the anode. Figure 7 displays the discharge capacity vs. the cycle number of the cell Li/BP-PSSPSI (EC/PC)/$LiFePO_4$ at the discharge rate of 0.1 C and room temperature. The discharge capacity of the cell is around 125 mAh g^{-1} for all the 15 cycles tested and the battery performance remained to be very stable. Of course, to gain thorough understanding of the electrolyte membranes, more extensive testing of the battery performance at various temperatures and charging/discharging rates needs to be performed. Nevertheless, the preliminary performance testing corroborates the viability of the proposed concept and confirms the electrochemical stability of the synthesized electrolyte membrane.

Journal of Materials Chemistry A Accepted Manuscript

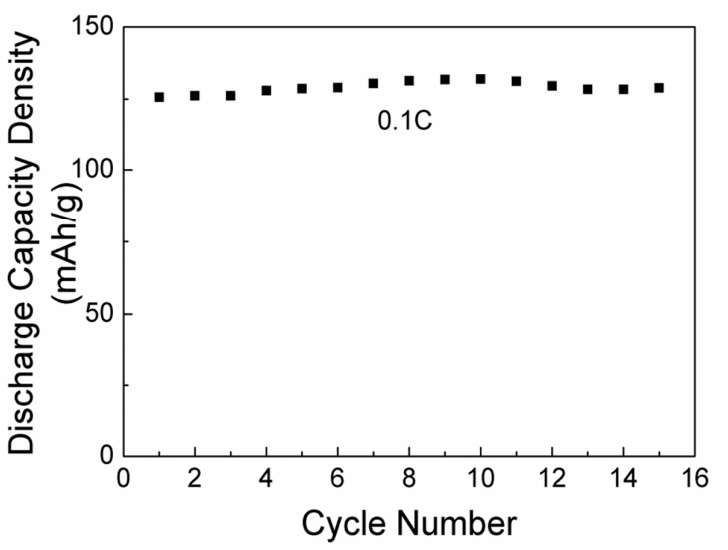

Figure 7. Cycle performance of the Li/BP-PSSPSI membrane (EC/PC)/ $LiFePO_4$, at room temperature and discharge rate of 0.1 C.

4. **Conclusions**

We present here a novel synthetic protocol for design of polystyrene-based single ion porous polymer electrolyte, which possesses high porosity with open and interconnected pores of meso and macro sizes. This enables selected functional groups to be placed on the walls of the pores. The sulfonyl(phenylsulfonyl)imide groups cling in the pores give rise to significant charge-delocalization in the framework, resulting in weak association of lithium ions in the extra-framework with the polymer. The large porosity of the material enables organic solvents conventionally used in Li-ion batteries to be accommodated, leading to high Li ion mobility with the ionic conductivity on the order of 10^{-3} Scm^{-1}, which is comparable to the conventional liquid electrolytes. The pore sizes are tunable and can be altered by using different silica particle synthesis methods. The mechanical problem associated with the brittleness of the material as well as the high porosity of membrane can be largely overcome by binding with a PVDF solution, which results in only slight reduction of conductivity as well as porosity. The electrolyte with the PVDF binder exhibits good thermal stability. The preliminary cell performance testing confirms the electrochemical stability of the electrolyte membrane and supports its suitability for applications in Li-ion batteries. Further understanding on the battery performance can be gained through extensive testing of the

Journal of Materials Chemistry A Accepted Manuscript

electrolyte membranes at a range of temperatures and charging/discharging rates, which is currently underway in our lab.

Acknowledgment

The authors gratefully acknowledge support of a Start-up grant from NUS, a POC grant from National Research Foundation of Singapore, Singapore–Peking-Oxford Research Enterprise (SPORE) and the National Natural Science Foundation of China (No. 21233006). We thank Prof. D. Zhao for his assistance of pore size measurement.

References

1. Choi, N.-S., et al., *Challenges Facing Lithium Batteries and Electrical Double-Layer Capacitors.* Angewandte Chemie International Edition, 2012. **51**(40): p. 9994-10024.
2. Etacheri, V., et al., *Challenges in the development of advanced Li-ion batteries: a review.* Energy & Environmental Science, 2011. **4**(9): p. 3243-3262.
3. Jeong, G., et al., *Prospective materials and applications for Li secondary batteries.* Energy & Environmental Science, 2011. **4**(6): p. 1986-2002.
4. Goodenough, J.B. and Y. Kim, *Challenges for Rechargeable Li Batteries†.* Chemistry of Materials, 2009. **22**(3): p. 587-603.
5. *www.batteryuniversity.com/index.php/learn/article/is_lithium_ion_the_ideal_battery*.
6. Scrosati, B., *Recent advances in lithium ion battery materials.* Electrochimica Acta, 2000. **45**(15–16): p. 2461-2466.
7. Väyrynen, A. and J. Salminen, *Lithium ion battery production.* The Journal of Chemical Thermodynamics, 2012. **46**(0): p. 80-85.
8. Croce, F., et al., *Advanced electrolyte and electrode materials for lithium polymer batteries.* Journal of Power Sources, 2003. **119-121**: p. 399-402.
9. Scrosati, B. and R. Neat, *Lithium polymer batteries*, in *Applications of Electroactive Polymers*, B. Scrosati, Editor. 1993, Springer Netherlands. p. 182-222.
10. *http://am.delphi.com/pdf/techpapers/2001-01-0959.pdf*.
11. Scrosati, B. and J. Garche, *Lithium batteries: Status, prospects and future.* Journal of Power Sources, 2010. **195**(9): p. 2419-2430.
12. Xu, K., *Nonaqueous Liquid Electrolytes for Lithium-Based Rechargeable Batteries.* Chemical Reviews, 2004. **104**(10): p. 4303-4418.
13. Ghosh, A., C. Wang, and P. Kofinas, *Block Copolymer Solid Battery Electrolyte with High Li-Ion Transference Number.* Journal of The Electrochemical Society, 2010. **157**(7): p. A846-A849.
14. Bouchet, R., et al., *Single-ion BAB triblock copolymers as highly efficient electrolytes for lithium-metal batteries.* Nat Mater, 2013. **12**(5): p. 452-457.
15. Lin, Y., et al., *A wider temperature range polymer electrolyte for all-solid-state lithium ion batteries.* RSC Advances, 2013. **3**(27): p. 10722-10730.
16. Feng, S., et al., *Single lithium-ion conducting polymer electrolytes based on poly[(4-styrenesulfonyl)(trifluoromethanesulfonyl)imide] anions.* Electrochimica Acta, 2013. **93**(0): p. 254-263.
17. *http://electronicdesign.com/energy/solid-polymer-electrolyte-makes-lithium-ion-safe.*
18. Song, J.Y., Y.Y. Wang, and C.C. Wan, *Review of gel-type polymer electrolytes for lithium-ion batteries.* Journal of Power Sources, 1999. **77**(2): p. 183-197.

Journal of Materials Chemistry A Accepted Manuscript

19. Manuel Stephan, A., *Review on gel polymer electrolytes for lithium batteries.* European Polymer Journal, 2006. **42**(1): p. 21-42.
20. *Advances in Lithium- Ion Batteries*, ed. B.S. Walter A. van Schalkwijik. 2002: Kluwer Academic Publishers.
21. Lin, K.-J., K. Li, and J.K. Maranas, *Differences between polymer/salt and single ion conductor solid polymer electrolytes.* RSC Advances, 2013. **3**(5): p. 1564-1571.
22. Agrawal, R.C. and G.P. Pandey, *Solid polymer electrolytes: materials designing and all-solid-state battery applications: an overview.* Journal of Physics D: Applied Physics, 2008. **41**(22): p. 223001.
23. Meziane, R., et al., *Single-ion polymer electrolytes based on a delocalized polyanion for lithium batteries.* Electrochimica Acta, 2011. **57**(0): p. 14-19.
24. Tian, L.-Y., X.-B. Huang, and X.-Z. Tang, *Single-ionic gel polymer electrolyte based on polyvinylidene fluoride and fluorine-containing ionomer.* European Polymer Journal, 2004. **40**(4): p. 735-742.
25. Sun, X.-G., C.L. Reeder, and J.B. Kerr, *Synthesis and characterization of network type single ion conductors.* Macromolecules, 2004. **37**(6): p. 2219-2227.
26. Watanabe, M., Y. Suzuki, and A. Nishimoto, *Single ion conduction in polyether electrolytes alloyed with lithium salt of a perfluorinated polyimide.* Electrochimica Acta, 2000. **45**(8–9): p. 1187-1192.
27. Zhu, Y.S., et al., *A new single-ion polymer electrolyte based on polyvinyl alcohol for lithium ion batteries.* Electrochimica Acta, 2013. **87**(0): p. 113-118.
28. Wang, X., et al., *A single-ion gel polymer electrolyte based on polymeric lithium tartaric acid borate and its superior battery performance.* Solid State Ionics, (0).
29. McOwen, D.W., et al., *Concentrated electrolytes: decrypting electrolyte properties and reassessing Al corrosion mechanisms.* Energy & Environmental Science, 2014.
30. Jiang, J., et al., *Gel polymer electrolytes prepared by in situ polymerization of vinyl monomers in room-temperature ionic liquids.* Reactive and Functional Polymers, 2006. **66**(10): p. 1141-1148.
31. Liao, C., X.-G. Sun, and S. Dai, *Crosslinked gel polymer electrolytes based on polyethylene glycol methacrylate and ionic liquid for lithium ion battery applications.* Electrochimica Acta, 2013. **87**(0): p. 889-894.
32. Sun, X.-G., et al., *Network Single Ion Conductors Based on Comb-Branched Polyepoxide Ethers and Lithium Bis(allylmalonato)borate.* Macromolecules, 2004. **37**(14): p. 5133-5135.
33. Sun, X.-G. and J.B. Kerr, *Synthesis and characterization of network single Iion conductors based on comb-branched polyepoxide ethers and lithium bis(allylmalonato)borate.* Macromolecules, 2005. **39**(1): p. 362-372.
34. Zhang, Y., et al., *A class of sp3 boron-based single-ion polymeric electrolytes for lithium ion batteries.* RSC Advances, 2013. **3**(35): p. 14934-14937.
35. Cho, T.-H., et al., *Battery performances and thermal stability of polyacrylonitrile nano-fiber-based nonwoven separators for Li-ion battery.* Journal of Power Sources, 2008. **181**(1): p. 155-160.
36. Liang, Y., et al., *Preparation and electrochemical characterization of ionic-conducting lithium lanthanum titanate oxide/polyacrylonitrile submicron composite fiber-based lithium-ion battery separators.* Journal of Power Sources, 2011. **196**(1): p. 436-441.
37. *http://www.fkf.mpg.de/565132/VI_02_13.pdf*.
38. Stöber, W., A. Fink, and E. Bohn, *Controlled growth of monodisperse silica spheres in the micron size range.* Journal of Colloid and Interface Science, 1968. **26**(1): p. 62-69.
39. Wang, H.-C., et al., *Analysis of Parameters and Interaction between Parameters in Preparation of Uniform Silicon Dioxide Nanoparticles Using Response Surface Methodology.* Industrial & Engineering Chemistry Research, 2006. **45**(24): p. 8043-8048.

Journal of Materials Chemistry A Accepted Manuscript

40. Chen, Y., et al., *Colloidal HPMO Nanoparticles: Silica-Etching Chemistry Tailoring, Topological Transformation, and Nano-Biomedical Applications.* Advanced Materials, 2013. **25**(22): p. 3100-3105.
41. Watanabe, R., et al., *Extension of size of monodisperse silica nanospheres and their well-ordered assembly.* Journal of Colloid and Interface Science, 2011. **360**(1): p. 1-7.
42. Shen, R., et al., *Polymeric Nanocapsule from Silica Nanoparticle@Cross-linked Polymer Nanoparticles via One-Pot Approach.* Nanoscale Research Letters, 2009. **4**(11): p. 1271 - 1274.
43. Khazaei, A., A. Mashak, and E. Mehdipour, *A Novel Synthesis and Characterization of 4-Acetylaminobenzene-p-styrene Sulphonate and its Polymer as Prodrug in Controlled Release Technique*, in *Iranian Polymer Journal* 1999. p. 115-121.
44. Shin, J.-P., et al., *Sulfonated polystyrene/PTFE composite membranes.* Journal of Membrane Science, 2005. **251**(1–2): p. 247-254.
45. Martins, C.R., G. Ruggeri, and M.-A. De Paoli, *Synthesis in pilot plant scale and physical properties of sulfonated polystyrene.* Journal of the Brazilian Chemical Society, 2003. **14**: p. 797-802.
46. Tanaka, Y. and Y. Tanaka, *Infrared spectra of bisaryl sulphonimide derivatives.* Chemical & Pharmaceutical Bulletin, 1974. **22**: p. 2546-2551.
47. Xiong, T., et al., *Remote amide-directed palladium-catalyzed benzylic C-H amination with N-fluorobenzenesulfonimide.* Chemical Communications, 2010. **46**(36): p. 6831-6833.
48. Yao, Q. and C.A. Wilkie, *Thermal degradation of blends of polystyrene and poly(sodium 4-styrenesulfonate) and the copolymer, poly(styrene-co-sodium 4-styrenesulfonate).* Polymer Degradation and Stability, 1999. **66**(3): p. 379-384.
49. *http://www.equflow.com/sites/default/files/bijlagen/bestanden/solef_hylar_2009.pdf*.
50. de C. Campos, J.S., A.A. Ribeiro, and C.X. Cardoso, *Preparation and characterization of PVDF/CaCO3 composites.* Materials Science and Engineering: B, 2007. **136**(2–3): p. 123-128.
51. Wang, J., *Analytical Electrochemistry* A John Wiley & Sons Inc., Publications.
52. Nagasubramanian, G., *Comparison of the thermal and electrochemical properties of LiPF6 and LiN(SO2C2F5)2 salts in organic electrolytes.* Journal of Power Sources, 2003. **119-121**: p. 811-814.
53. Voice, A.M., et al., *Thermoreversible polymer gel electrolytes.* Polymer, 1994. **35**(16): p. 3363-3372.
54. Geiculescu, O.E., et al., *Solid polymer electrolytes from polyanionic lithium salts based on the LiTFSI anion structure.* Journal of The Electrochemical Society, 2004. **151**(9): p. A1363-A1368.

Journal of Materials Chemistry A Accepted Manuscript